PHYSICAL REVIEW B VOLUME 17, NUMBER 12 15 JUNE 1978

Self-consistent electronic structure of the chlorine-adsorbed silicon (111) surface

Kenneth Mednick and Chun C. Lin

Department of Physics, University of Wisconsin, Madison, Wisconsin 53706

(Received 23 December 1977)

A first-principles self-consistent-field calculation of the electronic structure of the Si(111) surface with a layer of chemisorbed Cl atoms has been performed by means of the method of linear combinations of atomic orbitals. A thin-film crystal consisting of twelve infinite (111) Si layers plus one layer of Cl on each side is considered. The crystal potential is expressed as a superposition of localized function at each site, and the basis functions consist of two-dimensional Bloch sums of the $1s,2s,2p,3s,3p$ atomiclike functions and of contracted-Gaussian orbitals for each layer of the film. By means of the Gaussian techique, all the multicenter integrals are evaluated exactly and the Hamiltonian matrix elements are computed by summing these integrals over all the lattice points to convergence. The solution of the one-electron Hamiltonian is carried to self-consistency. Application of Mulliken's method of population analysis enables us to determine the fraction of electron charge allocated to each layer for a given wave function and quantitatively characterize the localization of the surface states. At the $\bar{\Gamma}$ point of the two-dimensional Brillouin zone, we find a surfacelike σ state at -13.4 eV (relative to the vacuum level) and a π surface state at -10.7 eV. The localized behavior of the latter persists at $\vec{k}_{\parallel}$ points on the $\bar{\Gamma}\bar{M}$ line. The calculated local density of states (LDS) for the valence band agrees well with the experimental photoemission data. In the lower conduction band we find one LDS peak due to surface states at -3.4 eV which corresponds closely to the electron-energy-loss data. Estimates of the LDS for the upper conduction band have been made and the results are in reasonable accord with experiment. A population-analysis calculation indicates a net charge of -0.35 e/atom (e being proton charge) for the Cl layer and 0.27 e/atom for the adjacent Si layer with some residual ionicity in the next few layers.

I. INTRODUCTION

In the last few years first-principles calculations of energy-band structure of solids based on the method of linear combinations of atomic orbitals (LCAO) have been quite successful for a variety of crystals including the alkali and transition metals, group-IV element crystals, aluminum, metal oxides, alkali halides, and polyethylene.[1-11] More recently application of this method has been extended to imperfect solids such as point-defect crystals[12,13] and amorphous Si.[14,15] The concept of LCAO indeed has been used, for many years, for qualitative description of the electronic structure of solids, and many empirical calculations based on techniques of parametrization have been performed. Nevertheless, the difficulty of evaluating the multicenter integrals which appear in the Hamiltonian matrix elements had rendered first-principles calculations prohibitively unrewarding. The recent success of the LCAO calculations may be attributed mainly to the introduction of the Gaussian-type orbitals (GTO).[16] When the atomic orbitals are expanded by the GTO's, all the multicenter integrals involving the kinetic and potential-energy terms can be either evaluated analytically or expressed in terms of the error function[14,17] so that one can readily compute the Hamiltonian matrix elements exactly by carrying out the lattice summation of these integrals to convergence. Techniques for self-consistent-field (SCF) calculations have been developed,[10,18] and theoretical Fermi surfaces, optical conductivities, and Compton profiles based on SCF LCAO band structures have been reported.[3,4,19]

In view of the surging interest in theoretical understanding of the electronic structure of solid surfaces,[20] it is natural to extend our LCAO scheme to chemisorbed surfaces. The superposition representation of the crystal potential not only provides a natural distinction between the substrate and adsorbate atoms, but also automatically reproduces the abruptness of the crystal surface. The multicenter integrals involved in the surface problem can be evaluated in the same manner as for the bulk crystal. The specific subject of our study is the case of the Si(111) surface with a layer of chemiadsorbed Cl atoms. Photoemission experiments for this system have been reported, and the effects of the Si-Cl interaction on the observed photoemission intensity delineated.[21,22] Also in Ref. 22 is a theoretical SCF calculation of the valence-band local density of states and an analysis of the peaks therein from the view point of Si-Cl bonding. Comparison between the theoretical results with the experimental data makes it possible to determine the site geometry of the adsorbate. The calculation given in Ref. 22 is based on the method of pseudopotential. In this paper we describe an SCF LCAO procedure for first-principles calculations of the electronic structure of the Cl-adsorbed Si(111) surface. The calculated energy spectrum for both the valence and conduction bands can be compared with the experimental data. Also the LCAO form of the wave functions enables one to analyze the electronic states in terms of the atomic characters and determine quantitatively the electronic charge distribution in the crystal.

For clean surfaces, self-consistent first-principles calculations of the electronic structure of crystals, infinite in two dimensions and either semi-infinite or finite in the third, have been performed by different methods.[20] The works of Appelbaum and Hamann deal with semi-infinite crystals; the electronic states are solved by the technique of scattered waves.[23] On the other hand, thin-film crystals (~10 layers) are used by Alldredge and Kleinman.[24] It is a common practice to stack a series of thin films with a constant distance between two adjacent ones sufficiently large so that the electronic charge density is virtually zero midway between two films. In this manner the crystal potential can be regarded to have a three-dimensional periodicity and therefore can be expressed in a Fourier series. Consequently the electronic wave functions can be handled by a plane-wave-like expansion.[24] The approach of Appelbaum and Hamann and that of Alldredge and Kleinman have since been applied to many different systems. In addition to the works by those two groups, studies of Cu(100) surface (three-layer film) and diamond (100) surface (a stack of 21-layer films) have been performed by the LCAO technique with Gaussian basis.[25,26] There are also first-principles SCF calculations for surfaces in which a finite cluster is used to simulate the solid; the methods of treatment there are quite different from those employed for solid surfaces of infinite extent.

As to first-principles theoretical calculations for surface adsorption, the method of Appelbaum and Hamann has been extended to the case of Si (111) with H atoms.[27] Non-SCF calculations on adsorption of O and CO on Ni surfaces have been performed by the method of linear combination of muffin-tin orbitals.[28]

Our treatment of the adsorption problem is based on the Hartree-Fock-Slater scheme. We consider a single thin film (14 layers) of solid which is infinite in two dimensions, but no quasi-periodicity in the third dimension is assumed. The one-electron Hamiltonian is solved by using LCAO-type basis functions in which the atomiclike orbitals are expanded by GTO. In computing the multicenter integrals involving the crystal potential, the Coulomb and exchange interaction of all the atoms in the solid are fully taken into account. By means of the Gaussian technique, all the multicenter integrals are evaluated exactly. The Hamiltonian matrix elements are expressed as a summation of the multicenter integrals over the infinite lattice sites which is carried out to convergence. An iteration scheme has been developed to carry the solution to self-consistency. As our starting point we first perform an SCF calculation for the bulk Si crystal. Although an SCF LCAO scheme has been previously developed for bulk crystals,[9,10] we have made some changes in the computational procedure so as to make it more directly adaptable to the adsorption problem. We will describe in some detail this SCF procedure for the bulk crystal in Sec. II, since much of the technique developed therein forms the foundation for the adsorption work. Following this will be an account of the computational method for the Si(111) Cl system. Presentation of the results, comparison with experiment, and discussion will be given in Secs. II–VI.

The term "method of tight binding" has been often used interchangeably with the LCAO method in bulk-crystal works. The name "tight binding" in surface work has been associated with the semi-empirical approach in which the Hamiltonian matrix elements are chosen by some empirical means and, usually, only include nearest-neighbor (and sometimes second-nearest-neighbor) interactions.[29,30] In the last few years, calculations based on this procedure have met with considerable success for clean surfaces, and it has been extended to chemisorbed systems.[31,32] Both the empirical tight-binding method and our method employ basis functions involving atomic orbitals, but we calculate the matrix elements from first principles and include interaction of an atom with all other atoms in the crystal regardless of their distances. Furthermore, our LCAO scheme provides the option of including additional basis functions (other than those associated with the occupied atomic shells) so that it is also applicable to the unoccupied conduction states.

II. SCF BAND CALCULATION OF THE BULK SILICON CRYSTAL

We designate the two interpenetrating face-center-cubic (fcc) sublattices of lattice constant a (5.429 Å) as 1 and 2 and choose our coordinate axes to be parallel to the cubic axes. The two sublattices are displaced from each other by $\vec{t}_2 - \vec{t}_1$, where $\vec{t}_2 - \vec{t}_1 = \frac{1}{4}a(1,1,1)$. From a given atomiclike orbital (such as $1s$, $2s$, $2px$, etc.), a Bloch sum can be constructed for each of the two sublattices. Instead of using the Bloch sums of the individual sublattices directly, we take as the basis functions the "plus" and "minus" combination, as is done in Ref. 7,

$$b_\alpha^\pm(\vec{k},\vec{r}) = I^\pm(\alpha) N^{-\frac{1}{2}} \sum_\nu e^{i\vec{k}\cdot\vec{R}_\nu}[\phi_\alpha(\vec{r}-\vec{R}_\nu-\vec{t}_1) \pm \phi_\alpha(\vec{r}-\vec{R}_\nu-\vec{t}_2)] , \quad (1)$$

where ϕ_α denotes a localized orbital, $\vec{R}_\nu$ is a translational vector of the fcc lattice, N is symbolically the number of unit cells in the crystal, and

$$\begin{aligned} I^+(\alpha) &= -iI^-(\alpha) = 1, \quad \text{when } \alpha \text{ is } s \text{ type}, \\ I^+(\alpha) &= -iI^-(\alpha) = i, \quad \text{when } \alpha \text{ is } p \text{ type}. \end{aligned} \quad (2)$$

The use of Eq. (1) as basis functions has the advantage of making all the matrix elements real. Although a common choice for ϕ_α is the set of occupied orbitals of the free atoms (1s-3p), higher accuracy can be achieved by using a series of single Gaussians of different widths for ϕ_α.[2,33] The use of single-Gaussian Bloch sums, however, entails a much larger basis set. To retain good accuracy with a moderately small basis set, we resort to the method of contracted Gaussians.[33,34] Following the procedure of Ref. 33, we solve the energy secular equation for $\vec{k}=0$ using a basis of 11 s-type and 11 p-type single-Gaussian Bloch sums of exponents 0.186 040, 0.257 644, 0.503 922, 1.452 21, 3.937 14, 12.8156, 30.6395, 77.6064, 214.004, 657.466, and 2330.01.[35] (Description of the crystal potential is given in the next paragraph.) According to the weightings of these Bloch sums in the 1s core-state eigenvector, we construct a linear combination of the Gaussians centered at the same site (called a contracted Gaussian) which is taken as the 1s "optimized orbital." A similar procedure is used for 2s and 2p. To generate the 3s and 3p optimized orbitals, we use, respectively, the Γ_{1v} and Γ'_{25v} eigenfunctions to form the contracted Gaussians. To these optimized orbitals, we add an s-type function [exp(−0.186 040 r^2) −exp(−0.257 644 r^2)] which is then orthogonalized to 1s, 2s, 3s, and a similar p-type function so as to improve the variational freedom; they are referred to as the s' and p' orbitals. By comparing eigenvalues of this 13-function set (which amounts to 26 basis functions because of two atoms per unit cell) to a larger pure single-Gaussian set involving 88 basis functions, we find that valence-band energies differ by no more than 0.08 eV and the energies of the bottom part of the conduction band by no more than 0.15 eV. One can also introduce some d-type Bloch sums for additional variational freedom. However, since we do not use d-orbitals in the surface adsorption work, they are not included in the bulk calculation.

In the earlier work of LCAO band calculation of diamond type crystals, the crystal potential was expanded in a Fourier series.[7] This technique made computation of matrix elements expedient, but is limited to systems with three-dimensional translational symmetry. In order to have a scheme applicable to systems of lower symmetry, we adopt the local decomposition representation for the crystal instead of employing Fourier expansion. This entails a considerable modification in the computational procedure to our SCF LCAO scheme for bulk crystal[10] published previously. In the present work the crystal potential is expressed as a lattice sum of local functions centered at each atom. These functions are chosen so that their range does not exceed two or three times the value of the associated atomic radius. Furthermore, the angular dependence must be chosen to be compatible with any rotational and mirror symmetries of the crystal. For silicon the angular dependence may be spherical or have the form xyz. Higher-order terms such as $[x^4+y^4+z^4-(\frac{3}{5})r^4]$ exist but are not included (justification for their omission will be given in the next paragraph). We have then,

$$V_{\text{cry}}(\vec{r}) = \sum_\nu \sum_{k=1,2} U_k(\vec{r}-\vec{R}_\nu-\vec{t}_k) , \quad (3)$$

$$U_1(\vec{r}) = U_s(r) + xyzU_{xyz}(r) , \quad (4)$$

$$U_2(\vec{r}) = U_s(r) - xyzU_{xyz}(r) . \quad (5)$$

The relationship between U_1 and U_2 is due to the glide-plane symmetry of silicon. Evaluation of multicenter integrals is greatly facilitated by expanding the localized potentials by Gaussians, i.e.,

$$U_s(r) = \sum_l (A_l/r)e^{-C_l r^2} + \sum_m \xi_m e^{-b_m r^2} , \quad (6)$$

with

$$\begin{aligned} &\sum_l A_l = -Z , \quad \sum_l A_l C_l = 0 , \\ &U_{xyz}(r) = \sum_n \xi'_n e^{-b'_m r^2} . \end{aligned} \quad (7)$$

The first summation in Eq. (6) allows for the r^{-1} singularity near each silicon nucleus. A typical multicenter integral appearing in the Hamiltonian matrix element involves the product of a Gaussian at site A, another at B, and U_s (or $xyzU_{xyz}$) centered at C. The integrals associated with the first summation in Eq. (6) can be expressed in terms of the error function and those associated with the remainder of (6) and $xyzU_{xyz}$ can be reduced to analytic form.

To start an SCF calculation we use the overlapping atomic potential (OAP) as the initial approximation of the crystal potential. In other words; the zeroth-order version of U_s (called $U_s^{(0)}$) is taken as the spherically averaged potential of a free Si atom computed from the atomic Hartree-Fock wave function with the statistical exchange approximation. Using the 13-function set we solve the secular equations $|H_{ij} - ES_{ij}| = 0$ to determine the one-electron energies and wave functions for four $\vec{k}$ points in the Brillouin zone (BZ), namely, Γ, X, L, and W. The first-order crystal electron density can be obtained by performing a numerical integration over the Brillouin zone using these four points. We calculate the electron density at 357 points in the fundamental wedge of the silicon crystal which has a volume of $\frac{1}{48}$ of the Wigner-Seitz cell. The electron density at points outside the wedge may be found by appropriate rotations and translations. The fundamental wedge is defined by

$$x \geqslant y \geqslant |z| \geqslant 0, \text{ with } x + y \leqslant \tfrac{1}{2}a, \tag{8}$$

and

$$\begin{aligned} &x + y + z < (3/8)a, \text{ if } y < a/8, \\ &x + y + z \leqslant (3/8)a, \text{ if } y \geqslant a/8. \end{aligned} \tag{9}$$

The crystal electron density is decomposed into a superposition of localized functions over the lattice points, i.e.,

$$\rho_{\text{cry}}(\vec{r}) = \sum_{\lambda} \sum_{k=1,2} \rho_k^a(\vec{r} - \vec{R}_\lambda - \vec{t}_k), \tag{10}$$

where ρ^a is determined from the calculated values of ρ_{cry} (at 357 points in the fundamental wedge) by means of a multicenter numerical curve fitting. Here ρ^a may contain a spherical part and an angular part including terms like xyz, $x^4 + y^4 + z^4 - (\frac{3}{5})r^4$, etc. However, we find that a good fit of Eq. (10) can be achieved by using only the spherical term (ρ_s^a) and the xyz term (ρ_{xyz}^a), hence no higher angular terms are included. The relations between ρ_s^a, ρ_{xyz}^a and ρ_1^a, ρ_2^a are similar to Eqs. (4) and (5). In fact the Coulomb component of the electronic part of U is determined by solving the Poisson equation with ρ^a. Since the only angular part of ρ^a is the xyz term, it is not necessary to carry U beyond this term. We have found it convenient to fit the electron density with functions like $(\alpha/\pi)(1.5 - \alpha r^2) e^{-\alpha r^2}$, $(\alpha/\pi)(4.5 - \alpha r^2)xyze^{-\alpha r^2}$, and $(\alpha/\pi)(\alpha r^2 - 0.5) e^{-\alpha r^2}/r$ as they yield Coulomb potentials of the form $e^{-\alpha r^2}$, $xyze^{-\alpha r^2}$, and $(1 - e^{-\alpha r^2})/r$, respectively. For $\rho^a(\vec{r})$ we use eleven terms of the first kind, two terms of the second kind, and two terms of the third. The two $1/r$-type terms must be constrained, as stated in the auxiliary conditions of Eq. (6) so that the electronic Coulomb potential approaches $-Z/r$ as $r \to 0$ and $\rho(0)$ remains finite.

The exchange part of the crystal potential is handled by the statistical approximation. Since $[\rho_{\text{cry}}(\vec{r})]^{1/3}$ is not equal to the sum of $(\rho)^{1/3}$, it is necessary to separately fit $\rho_{\text{cry}}{}^{1/3}$ from the calculated values for 357 points into a lattice superposition form as

$$[\rho_{\text{cry}}(\vec{r})]^{1/3} = \sum_{\lambda} \sum_{k=1,2} g_k(\vec{r} - \vec{R}_\lambda - \vec{t}_k). \tag{11}$$

A multicenter, nonlinear fit is performed using terms like $e^{-\alpha r^2}$ and $(xyz)e^{-\alpha r^2}$ (ten of the former and two of the latter). Again g_1 and g_2 assume the form of Eqs. (4) and (5). The U functions are composed of the contributions from the nuclear charge, the electronic Coulomb term, and the exchange term as

$$\begin{aligned} U_k(\vec{r}) = -\frac{Z}{r} + \int [\rho_k^a(\vec{r}\,')/|\vec{r} - \vec{r}\,'|]d\tau' \\ -3\alpha(3/8\pi)^{1/3} g_k(\vec{r}),\ k = 1, 2. \end{aligned} \tag{12}$$

If ρ^a and g were handled the way described above, the integral in Eq. (12) would generate a Z/r term to cancel the first term so that U_k is in the Gaussian form as depicted in Eqs. (6) and (7). From the first-order electron density one generates the first-order U and V_{cry}. Solution of the secular equations based on this potential yields the second-order electron density and the iteration process is repeated until self-consistency is reached. During each iteration the contraction coefficients for the Gaussians in the $1s, \ldots, 3p$ optimized orbitals are recalculated in accordance with the new Hamiltonian so as to allow for orbital relaxation. Since curve fitting is used extensively in our computation, it is important to ascertain whether the calculated energies depend in any appreciable way on the curve fitting. To this end we perform another fit for Eqs. (10) and (11) using an entirely different kinds of localized functions. The difference in the resulting energies is typically 0.02 eV. All the functions determined by curve fit, such as $\rho^a(\vec{r})$, and $g(\vec{r})$, ultimately appear in the multicenter integrals, thus fluctuations due to slightly inexact fitting are evened out by the integration and would have a very small effect on the matrix elements.

In our calculation of V_{cry}, absolute potential is used throughout without any additive constants. Therefore the energy eigenvalues are referred to the vacuum level. Our SCF LCAO calculation for LiF shows that one can get accurate vacuum levels relative to the valence band.[10]

We first chose $\alpha = 1$ for the parameter in the exchange approximation. The SCF calculation with the 13-function set gives the top of the valence band at 6.36 eV below the vacuum level and an indirect band gap of 1.43 eV. They are larger than the corresponding experimental values of 5.15 and 1.16 eV.[36,37] Our calculated indirect gap is also slightly larger than the value of 1.10 eV obtained by the SCF orthogonalized-plane-waves (OPW) method.[38] (Augmentation of our basis set by single Gaussians decreases the band gap to 1.37 eV which is still larger than the OPW value. The OPW scheme of Ref. 38 involves some approximations associated with dividing the states into valence states and core states and with the way the core states are treated. However, we have not investigated whether they can account fully for the discrepancy. No vacuum-level energies are given in Ref. 38.) With $\alpha = 0.90$ in our SCF calculation, the top of the valence band lies 5.19 eV below the vacuum level and the indirect band gap becomes 1.17 eV. The vacuum level plays a very important role in surface problems. An incorrect energy separation between the valence band and the vacuum level for the limiting bulk crystal would affect the surface-adsorption states and obscure the comparison between theory and experiment. For this reason we adopt $\alpha = 0.90$ for the bulk Si crystal. (Additional discussion will be given in Sec. VI.)

III. METHOD OF CALCULATION FOR SURFACE ADSORPTION

The crystal under consideration is a (111) slice from an infinite silicon crystal with one layer of Cl atoms opposite to each surface Si atom such that the Si-Cl bonds are perpendicular to the surface. This structure has been confirmed by the experiment of Rowe *et al.*[21] The single-bond length for Si-Cl is quite constant for a number of molecules, being 2.050 Å for SiH_3Cl, 2.021 Å in $SiHCl_3$, 2.021 Å in CH_3SiCl_3, and 2.01 Å in Si_2Cl_6.[39] Accordingly we choose the Si-Cl distance as 2.032 Å for our problem. It is assumed that the outer layers of Si atoms are not relaxed from their infinite-crystal positions. This assumption is reasonable because the Si-Cl bonds stabilize the boundary Si atoms, as opposed to the case of clean surfaces where layer relaxation is an important factor. We choose the z axis to be normal to the surface. Each layer, which is infinite in two dimensions, possesses the same translational invariance, but different layers may be displaced from each other as shown in Fig. 1. To fully specify the location of the atoms in the nth layer, we need only give the position ($\vec{T}_n$) of one of its constituent atoms. All other atoms of this layer can then be obtained through the two-dimensional translation vectors $\vec{R}_\lambda$. For this work, we take a film consisting of 12 layers of Si plus an overlayer of Cl on each side. One of the Cl layers is designated as $n = 7$, and one on the opposite side as $n = -7$. The adjacent Si layers are $n = 6$ and $n = -6$, etc. In this labeling system there is no layer corresponding to $n = 0$. The vectors $\vec{T}_7$, $\vec{T}_6$, $\vec{T}_5$, $\vec{T}_4$, $\vec{T}_3$, $\vec{T}_2$, and $\vec{T}_1$ are, respectively, (all in Å), (0, 0, 10.260), (0, 0, 8.228), (0, 2.216, 7.445), (0, 2.216, 5.094), (0, −2.216, 4.310), (0, −2.216, 1.959), and (0, 0, 1.175). Other layers may be found by inversion through the origin, e.g., $\vec{T}_{-2} = (0, 2.216, -1.959)$. Because the potential is written in a direct-space representation rather than as a Fourier series, it is not necessary to stack identical films along the z direction to produce a quasi-three-dimensional periodicity.

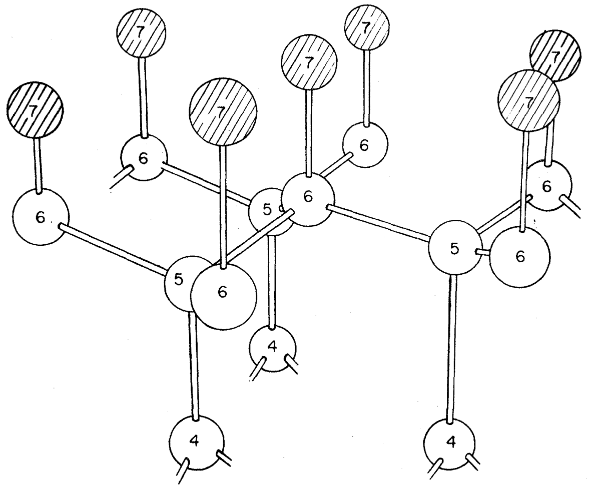

FIG. 1. Atomic-position structure of the Si(111) surface with one layer of adsorbed Cl atoms. The numeral 7 denotes the Cl atoms, 6 denotes the adjacent layer of Si atoms, 5 denotes the atoms in the next layer, and so forth.

The general procedure is to (i) select a set of basis functions; (ii) construct an initial crystal potential to start the SCF calculation; (iii) compute the matrix elements for this potential and solve the secular equations; and (iv) from the solution of the initial Hamiltonian, generate an improved Hamiltonian and iterate to self-consistency. The major guideline is that in the LCAO basis functions the atomiclike functions are expressed in GTO and that the crystal Hamiltonian is decomposed into a superposition of local functions which are in Gaussian form, analogous to Eqs. (3)–(7). (A description for each major step is given in Secs. III A–III C.)

A. Basis functions

Conforming to the planar translational symmetry of the crystal, we characterize an electron state by a two-dimensional wave vector $\vec{k}_{\parallel}$. The layer

Bloch sum for the nth layer of atoms is

$$B_{n,j}(\vec{k}_{\parallel}, \vec{r}) = \frac{1}{\sqrt{N}} \sum_{\lambda} e^{i\vec{k}_{\parallel}\cdot(\vec{R}_{\lambda}+\vec{T}_n)} \phi_j(\vec{r}-\vec{R}_{\lambda}-\vec{T}_n), \qquad (13)$$

where N is symbolically the number of atoms in the layer, and the local functions ϕ_j are the atomiclike orbitals of the Si and Cl atom expressed in Gaussians. For Si atoms, ϕ_j covers $1s$, $2s$, $2p$, $3s$, $3p$, s', and p' contracted Gaussian orbitals employed in the SCF band calculation of the bulk crystal. In the case of Cl we identified ϕ_j as the $1s$, $2s$, $2p$, $3s$, and $3p$ atomic wave functions, expanded in the same set of Gaussians as used for Si, plus an s' and p' orbital formed in the same way as their Si counterparts. This gives us 13 Bloch sums for each layer, hence a total of 182 basis functions. The Hamiltonian matrix elements between two $B_{n,j}$ functions, are in general, complex; this makes the secular equations difficult to handle. However, taking advantage of the inversion symmetry of the thin film, one can find a set of basis functions $B^{\pm}_{n,j}$ for which all matrices are real, i.e.,

$$B^{\pm}_{n,j}(\vec{k}_{\parallel}, \vec{r}) = I^{\pm}(j)[B_{n,j}(\vec{k}_{\parallel}, \vec{r}) \pm B_{-n,j}(\vec{k}_{\parallel}, \vec{r})], \qquad (14)$$

where $I^{\pm}(j)$ are given by Eqs. (2) if one replaces α by j therein.

B. Initial crystal potential

In the SCF calculation for the bulk crystal, we take the OAP as the starting potential. However, for the adsorption problem, the OAP approximation is not a good choice as a starting point, for, if it is so used, both the adsorption features and the bulk silicon features must be taken to self-consistency simultaneously. We find it advantageous to separate the bulk SCF work from the adsorption SCF work. To this end we take the infinite-crystal SCF potential derived from Sec. II and decompose it into a lattice sum of localized potentials for each Si atom in the form of Eq. (3). The starting potential for the thin-film problem is a direct superposition of this localized potential for each Si atom in the film and an atomiclike potential for each Cl atom on the two overlayers. This starting potential has the advantage that it already gives the correct SCF behavior for the interior part of the film. Consequently as we iterate the solution toward self-consistency, we find appreciable change in the electron density only near the surface of the thin film; hence, SCF interaction need be done for only a few layers near the two surfaces rather than the whole film.

C. SCF procedure

Since the starting potential is a superposition of localized potentials which are in the Gaussian form like Eqs. (6) and (7), the Hamiltonian matrix elements can be computed exactly as all their constituent multicenter integrals can be either evaluated in analytic form or expressed in terms of the error function. The energy levels and wave functions are determined by solving the secular equations for several $\vec{k}_{\parallel}$ points in the irreducible part of the two-dimensional BZ. In order to obtain the next improved crystal potential, we first compute the electron density of the film ρ_f by a numerical integration over $\vec{k}_{\parallel}$, i.e.,

$$\rho_f^{(1)}(\vec{r}) = \sum_{i,\vec{k}} \omega(\vec{k}_{\parallel}) g_i(\vec{k}_{\parallel}) |\psi_i(\vec{k}_{\parallel}, \vec{r})|^2, \qquad (15)$$

where ψ_i stands for the one-electron wave function for the ith band, $g_i(\vec{k}_{\parallel})$ is 0 or 2 depending on whether the state is empty or fully occupied, and $\omega(\vec{k}_{\parallel})$ is the weighting of the particular $\vec{k}_{\parallel}$ point in the two-dimensional integration. The superscript in ρ_f indicates that it is the first-iteration result. Here we use three points $\bar{\Gamma}$, $\bar{M}$, and $\bar{K}$ as shown in Fig. 2, with weightings of 0.25, 0.50, and 0.25, respectively. (The high-symmetry points in the two-dimensional BZ are designated by letters with a bar to distinguish them from the symbols for the three-dimensional BZ.) It is interesting to compare $\rho_f^{(1)}$ with the electron density corresponding to the Coulomb part of the initial potential described in Sec. III B. The latter, referred to as $\rho_f^{(0)}$, is simply a superposition of ρ_k^a [derived from the SCF bulk calculation as defined by Eq. (10)] at each Si site and a free-atom Cl charge density at each Cl site in the thin film. As expected, $\rho_f^{(1)}$ and $\rho_f^{(0)}$ are found to differ appreciably only in the surface region. Therefore, we curve fit their difference as a summation of localized functions over the atomic sites on the three outer layers on each side of the film, ($n = 7$, 6, 5, -5, -6, -7); viz.,

$$\rho_f^{(1)}(\vec{r}) - \rho_f^{(0)}(\vec{r}) = \sum_{n=\pm5,\pm6,\pm7} \sum_{\lambda} u_n(\vec{r}-\vec{R}_{\lambda}-\vec{T}_n). \qquad (16)$$

The localized function $u_n(\vec{r})$ is, of course, layer dependent. Furthermore, it may contain any angular component that is compatible with the point group C_{3v}. Thus the u functions are taken to have

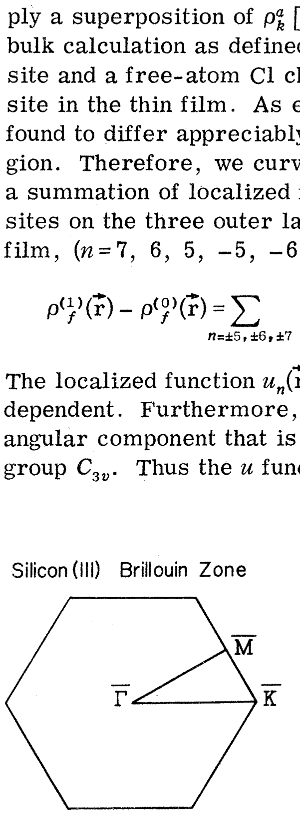

FIG. 2. Two-dimensional Brillouin zone of the Si(111) surface.

the general form[40]

$$u(\vec{r}) = f_0(r) + zf_1(r) + (2z^2 - x^2 - y^2)f_2(r) + z(2z^2 - 3x^2 - 3y^2)f_{31}(r) + y(y^2 - 3x^2)f_{32}(r) . \tag{17}$$

Truncation of this angular expansion is justified by the success of a good fit. We express the radial factors as

$$f_i(r) = \sum_j a_{ij} r^j e^{-\gamma_i r} . \tag{18}$$

The parameters a_{ij} and γ_i are to be determined by fitting Eq. (16). The exponential factor in Eq. (18) makes $u_n(\vec{r})$ a localized function; γ is generally around 3. For $f_0(r)$ two damping factors are used, one exponent about 3 and the other about 12. The degree of the polynomials is no greater than 5. From the electron density we obtain the corresponding Coulomb part of the thin-film potential by solving the Poisson equation,

$$[V_f^{(1)}(\vec{r}) - V_f^{(0)}(\vec{r})]_{\text{Coul}} = \sum_{n=\pm5,\pm6,\pm7} \sum_\lambda \int \left[\frac{u_n(\vec{r}\,' - \vec{R}_\lambda - \vec{T}_n)}{|\vec{r} - \vec{r}\,'|} \right] d\tau' . \tag{19}$$

It is easy to show that the integral on the right-hand side has the same angular dependence as u_n, so that we write

$$\int [u_n(\vec{r}\,')/|\vec{r} - \vec{r}\,'|]d\tau' = F_{n,0}(r) + zF_{n,1}(r) + (2z^2 - x^2 - y^2)F_{n,2}(r) + z(2z^2 - 3x^2 - 3y^2)F_{n,31}(r) + y(y^2 - 3x^2)F_{n,32}(r) , \tag{20}$$

where the F's can be expressed in analytic exponential form. To facilitate multicenter integration, it is expedient to cast the F's in a Gaussian version by means of curve fitting as

$$F_i = \sum_j \zeta_{i,j} e^{-\beta_{i,j} r^2} . \tag{21}$$

Similarly the new exchange potential, which is equal to $-3\alpha(3/8\pi)^{1/3}[\rho_f^{(1)}(r)]^{1/3}$, differs from the initial exchange potential only in the near-surface region so that their difference is again fitted to a superposition of another set of localized functions near a few outerlayers,

$$[V_f^{(1)}(\vec{r}) - V_f^{(0)}(\vec{r})]_X = \sum_{n=\pm5,\pm6,\pm7} \sum_\lambda v_n(\vec{r} - \vec{R}_\lambda - \vec{T}_n) , \tag{22}$$

where the subscript X designates the exchange part of the potentials involved. Like the electron-density difference, we find it sufficient to retain only the following terms in the angular expansion:

$$v_n(\vec{r}) = G_{n,0}(r) + zG_{n,1}(r) + (2z^2 - x^2 - y^2)G_{n,2}(r) + z(2z^2 - 3x^2 - 3y^2)G_{n,31}(r) + y(y^2 - 3x^2)G_{n,32}(r) , \tag{23}$$

where the G functions have the usual Gaussian form

$$G_i(r) = \sum_j \zeta'_{i,j} e^{-\beta'_{i,j} r^2} , \tag{24}$$

with the parameters ζ' and β' to be determined by fitting Eq. (23). For statistical stability in the curve-fitting procedure, we evaluate the electron density at many more nonequivalent points (945) than the number of parameters. The first-iteration correction to the crystal potential for the thin film is then

$$V_f^{(1)}(\vec{r}) - V_f^{(0)}(\vec{r}) = [V_f^{(1)}(\vec{r}) - V_f^{(0)}(\vec{r})]_{\text{Coul}} + [V_f^{(1)}(\vec{r}) - V_f^{(0)}(\vec{r})]_X . \tag{25}$$

Its matrix elements can be computed readily because both the Coulomb and exchange components are put in the Gaussian form through Eqs. (19)–(24). Once the solution of the first-iteration Hamiltonian is obtained, the entire procedure is repeated to reach self-consistency.

For the potential associated with the Si atoms, we adopt the value of 0.90 for the statistical exchange parameter as explained in Sec. II. As for the Cl atoms, we adhere to the conventional choice of $\alpha = 1$. The use of multivalue α for molecular systems in $X\alpha$-SCF calculations has been done frequently.[41] To allow for the different values of α in our problem, rather than dividing the crystal charge density of the thin film into a portion belonging to Si atoms and one to the Cl atoms, we use a position-dependent α defined as

$$\alpha = 0.90 \text{ for } |z| < 9.292 \text{ Å}, \qquad \alpha = 1.00 \text{ for } |z| > 9.292 \text{ Å} , \tag{26}$$

where the z coordinate of the electron is measured relative to the plane midway between the $n = 1$ and $n = -1$ layers. (A discussion of the effect of the choice α on the energy results is given in Sec. VI.)

IV. RESULTS: ANALYSIS OF THE ELECTRONIC STATES

An advantage of the LCAO representation of wave functions is that it displays directly the atomic orbital character and the interatomic bonding without the need of making an electron contour plot. Furthermore, for a given wave function, one can associate a fractional electron population to each atom by adopting the criterion of Mulliken.[42] To illustrate the essential idea, let us consider a triatomic molecule whose atoms are at points A, B, and C, with a one-electron LCAO molecular orbital

$$\psi = a\phi_A + b\phi_B + c\phi_C , \tag{27}$$

where ϕ_A is a normalized atomic orbital centered at A. The integrated electron density is then

$$\langle\psi|\psi\rangle = 1 = a^2 + b^2 + c^2 + 2ab\langle\phi_A|\phi_B\rangle + 2bc\langle\phi_B|\phi_C\rangle + 2ac\langle\phi_A|\phi_C\rangle . \tag{28}$$

Clearly a^2, b^2, and c^2 should be associated with the atoms at A, B, and C, respectively. The cross term $2ab\langle\phi_A|\phi_B\rangle$ is divided equally between A and B so that the fractional electron attributed to the atom at A is $a^2 + ab\langle\phi_A|\phi_B\rangle + ac\langle\phi_A|\phi_C\rangle$. This way of partitioning electron charge has been applied to molecules with great success.[42] For surface adsorption systems we can use it to determine the charge associated with the adsorbate and substrate atoms. This gives us a clear criterion for identifying the surface states as well as quantitatively characterizing their degree of localization. In this section we examine the individual states that are closely associated with the surface adsorption. By applying the Mulliken population analysis,[42] we determine the ionicity of the Cl and Si atoms in different layers.

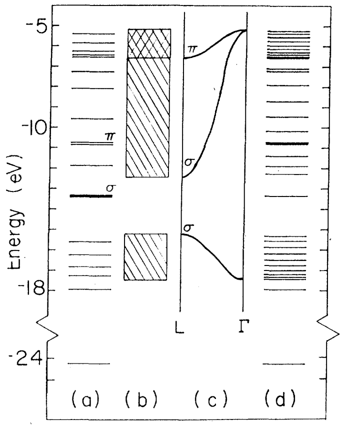

FIG. 3. In column (a) are the occupied $\bar{\Gamma}$- point energy levels of a thin film consisting of 12 layers of Si(111) and one Cl overlayer on each side. The same kind of levels of a film with 24 layers of Si(111) and one Cl overlayer on each side are given in column (d). Column (b) shows the coverage of the valence-band levels of the bulk Si crystal along the $\Gamma\Lambda L$ line of the three-dimensional BZ; the splitting of the s-pz and px-py branches is illustrated in column (c). The vacuum level is taken as the zero-energy reference.

A. $\bar{\Gamma}$ point

To gain insight into the properties of the surface-like states, we first focus our attention to the $\bar{\Gamma}$ points ($\vec{k}_\parallel = 0$) because the symmetry of this $\vec{k}_\parallel$ point makes the analysis of the electronic states simpler. Column a of Fig. 3 shows the occupied energy levels obtained for $\vec{k}_\parallel = 0$. Since the z axis for the surface problem is taken along the [111] direction of the fcc lattice, the $\bar{\Gamma}$ point in the two-dimensional BZ may be correlated with the [111] line (referred to the cubic axes) in the three-dimensional reciprocal space. For comparison, we also exhibit in Fig. 3 (column b) the valence-band levels of the bulk Si crystal for all $\vec{k}$ points on [111]. A gap within the valence states arises because we include only the states along the Λ line of the BZ. This is illustrated by the $\Gamma\Lambda L$ part of the energy-band diagram which is shown in column c of Fig. 3. The most noticeable differences between columns a and b are the levels in the forbidden regions of the bulk crystal, −24.2 and −13.4 eV. For each of these energies there are two nearly degenerate levels due to the two surfaces of the film, but we need only discuss one of each pair. The state at −24.2 eV is highly localized at the Cl layer consisting of predominately Cl 3s orbitals with little 3pz admixture. The electron distribution has a weighting of 0.91 and 0.09 for layers 7 and 6, respectively, and zero for layers 5–1. The state at −13.4 eV also has its major electron concentration at the Cl layer, but is somewhat less localized than the previous one, the distribution weighting for layers 7–4 being 0.53, 0.18, 0.16, and 0.04, respectively. This state is truly a surface state (rather than a surface-resonance state) because there are no bulk states of the same symmetry near that energy. The wave function at the Cl sites has a large 3pz component with some 3s mixing, and shows bonding (σ type) with the adjacent Si layer. The state at −18 eV in column a is slightly below the bulk valence-band limit indicating some distortion due to the surface overlayer.

To make further analysis of the thin-film and bulk states, it is convenient to classify them according to irreducible representations of the C_{3v} point group. [The thin film has an additional inversion symmetry which merely introduces a (+) or (−) label as in Eq. (14) and does not affect our analysis.] These energy levels shown in Fig. 3 are of either A_1-type (s, pz) or E-type (px, py). From Fig. 3(c) we see that the E levels (valence band) of the bulk states are confined to the energy range of −5.19 to −6.60 eV. The thin film, however, has sets of E doublets (four states altogether) at −10.7 eV which are well below the −6.60 eV limit and whose electron distribution on layers 7 and 6 are

0.91 and 0.08, respectively. These π-like states are weakly bonded with respect to the Cl and the adjacent Si atoms. They lie much below the energy limits within which E states may propagate through the infinite crystal and hence are forced to be localized on the surface. We get two sets of localized E doublets because of the two surfaces of the film; the two sets are, of course, virtually degenerate. No other $\overline{\Gamma}$ thin-film states show very strong preference to the Cl atoms. The A_1 states immediately above the localized level at −24.2 eV and the E states immediately above the localized π levels have small electron densities near the Cl atom, but are mostly concentrated at layers 6 and 5.

It is important to ascertain whether a 14-layer film is sufficiently thick to reproduce the bulk features of the crystal and to isolate one surface from the other. For this purpose we repeat the calculation for the $\overline{\Gamma}$ point using a 26-layer thin film (24 layers of Si with one layer of Cl on each side). The energy levels are shown in column d of Fig. 3. The σ and π surface states are now at −13.37 eV and −10.76 eV, respectively, as compared to −13.38 and −10.74 eV for the 14-layer calculation. There are, of course, more levels in column d than in column a because of the 12 extra layers of Si, but the general patterns are very much alike. As remarked before, each surface state occurs as a nearly degenerate pair because of the two surfaces of the film. The energy splitting of such a pair is a measure of the interaction between the two surfaces in the film for the particular surface state. For the 14-layer calculation the splittings of the surface π state is less than 0.0005 eV and that for the σ state at −13.4 eV is 0.09 eV. The latter is larger because it is less localized on the surface and the splitting is due to the small residual amplitudes near the $n=1$ layers. Upon enlarging the film to 26 layers, this residual amplitude diminishes; indeed the σ-state splitting becomes 0.003 eV.

B. The $\overline{\Gamma M}$ line

Along the $\overline{\Gamma M}$ line there is a mirror symmetry; hence, the energy levels can be labeled by A_1 (s, pz, and $\frac{1}{2}\sqrt{3}px+\frac{1}{2}py$) and A_2 ($-\frac{1}{2}px+\frac{1}{2}\sqrt{3}py$). Again, a thin-film A_2 level occurs below the energy limit of the A_2 bulk states so that it remains a true surface state. The A_1 states can couple with s and pz functions of the lower layers, thereby penetrating into the interior of the crystal. Thus, the surface π state at $\overline{\Gamma}$ splits into a true surface state A_2 and a surface-resonance state A_1 along the $\overline{\Gamma M}$ line. At the $\overline{M}$ point, the A_2 component is at −11.1 eV with a population of 0.83 at the Cl layer and 0.15 and 0.02 for the next two Si layers, whereas the distribution weights for the A_1 member (−11.4 eV) at $n=7$ through $n=4$ are 0.72, 0.04, 0.16, and 0.03. Both the surface type A_1 and A_2 levels occur in nearly degenerate pairs. The surface σ-like level (−13.4 eV at $\overline{\Gamma}$) becomes contaminated by px, py admixture at $\overline{M}$. As a result, one finds several levels with appreciable population at Cl, but none shows the same degree of localization as the σ state at $\overline{\Gamma}$. (Similar analyses can be performed for the surface states at other $\bar{k}$ points, but will not be detailed here.)

C. Ionicity of the adsorbate-substrate interface

For a given one-electron wave function we can assign a certain fraction of its charge to each layer of the atoms. When this is done for all occupied wave functions, the electronic charge, hence ionicity, for each atom may be determined. This requires an integration of all the $\vec{k}_\parallel$ states over the BZ which we replace by a summation over 15 $\vec{k}_\parallel$ points. To each point we assign a weighting factor which is proportional to the part of the area of the BZ that is closest to the $\vec{k}_\parallel$ point in question. This calculation gives the number of valence electrons per atom for layers 7–1 as 7.35, 3.73, 4.17, 3.90, 3.91, 3 96, and 3.98. We see a 0.35 unit of negative charge on Cl in line with the higher electronegativity of Cl over Si. The outermost Si layer shows a net +0.27 unit of charge. The remaining numbers signify that some residual ionicity permeates to as far as layer 3.

V. RESULTS: DENSITY OF STATES AND COMPARISON WITH EXPERIMENT

The density of states (DOS) is given by a numerical integration over the BZ,

$$D(\epsilon)=\sum_i \int \delta(E_i(\vec{k}_\parallel)-\epsilon)\,d\vec{k}_\parallel\,, \tag{29}$$

by means of a triangular integration scheme. The fundamental wedge of the BZ is partitioned into a number of small triangles. At the corners of each triangle, the energies are determined from the secular equation. We then approximate each energy band to be of the form $E(k_x, k_y)=a+bk_x+ck_y$ inside a triangle. Specifying an energy ϵ determines a unique line in the k plane. The DOS for that triangle and that energy is proportional to the length of the line enclosed by the triangle. The DOS for each triangle and each band is summed to yield the total DOS. We first performed the calculation with 164 triangles or 45 $\vec{k}_\parallel$ points and found the results to be nearly identical to those using 16 triangles or 15 $\vec{k}_\parallel$ points. Some noise is introduced by approximating the smooth bands with faceted surfaces. This is removed with a smoothing process in which we consider the DOS as a histogram of vertical strips centered at energy ϵ_0, $\Delta\epsilon$ wide and h_i high, and replace each strip by a normal distribution of area $h_i\Delta\epsilon$,

$$h(\epsilon)=(h_i\Delta\epsilon/\sqrt{2\pi}\sigma)\exp[-(\epsilon-\epsilon_0)^2/2\sigma^2]\,. \tag{30}$$

In our calculation, $\Delta\epsilon$ is chosen as 0.01 eV while σ is taken as 0.1 eV.

For the calculation of the local density of states (LDS), the weighting of the jth basis function (a layer Bloch sum) in the ith band must be determined. The LDS for the jth basis function is then defined through this weighting function as

$$D_j(\epsilon)=\sum_i\int w_{ij}(\vec{k}_\parallel)\delta(E(\vec{k}_\parallel)-\epsilon)\,d\vec{k}_\parallel\,. \tag{31}$$

In the triangular integration scheme the weighting function for a given band is taken as a constant, independent of $\vec{k}_\parallel$ throughout the small triangle, equal to the average of the values at the three corner points. The determination of the weighting function is again based on Mulliken's criterion[42] cited in Sec. IV, namely,

$$w_{ij}=V_{ji}^*\sum_l S_{jl}V_{li}\,, \tag{32}$$

where S_{jl} is the overlap matrix element between the jth and lth basis functions and V_{li} is the coefficient of the lth basis function in the ith band wave function. To get the LDS for a given layer, we sum $D_j(\epsilon)$ over all basis functions associated with that layer.

Experimental work on ultraviolet photoemission spectroscopy for the Si(111)Cl system has been performed by Rowe *et al.*[21] Their photoemission intensity reflects the LDS if one neglects the matrix-element effects. (In the following subsections we will present our calculated LDS and compare with the photoemission data.)

A. LDS for the valence band

In Fig. 4 are displayed the LDS for the Cl layer, Fig. 4(a); the LDS for the Cl plus the first (adjacent) Si layer, Fig. 4(b); and the LDS for the Cl plus the first and second Si layer, Fig. 4(c). Inspection of these curves reveals two dominant peaks at 11.2 and 13.4 eV below vacuum. The persistence of these two peaks in all three curves indicate that they are closely related to the Cl atoms. Indeed, they correspond, respectively, to the localized π state and the localized σ state at $\bar{\Gamma}$ as discussed in Sec. IV A. Of course each peak contains energy levels from different parts of the BZ, so the σ and π description is only approximate. We have seen in Sec. IV B that along the $\overline{\Gamma M}$ line the surface π states remain localized and undispersive whereas the σ state picks up small px and py constituents and becomes diffusive. This is reflected by the large difference in height between the two peaks. Their energies are in very good agreement with the two prominent peaks in the photoemission data[21] (peak C at −10.9 eV and peak B at −13.0 eV, both expressed relative to the vacuum level). In addition we find two broad peaks in the LDS, one at −8.7 eV and one at −16 eV. They are inconspicuous in Fig. 4(a), but become better developed as more Si layers are added. For this reason we attribute them to the bulklike states. We also see reasonable correspondence between our two bulklike peaks and the observed peaks D (−8.2 eV) and A (−14.9 eV) in the photoemission data.[21] The same kind of identification for the four observed peaks in terms of the bulklike states (A and D) adsorbate σ and π states (B and C) has been suggested in Refs. 21 and 22. The ultraviolet photoemission data reported by Pandey, Sakurai, and Hagstrum[32] shows a main peak at −10.7 eV and three smaller peaks at −7.5, −13.0, and −15.7 eV which are in good agreement with our LDS results.

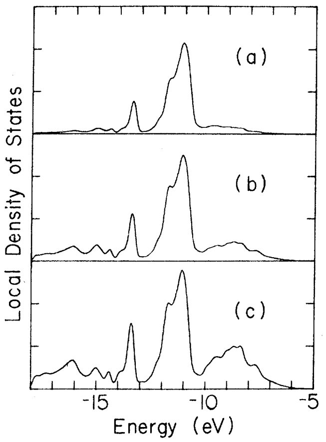

FIG. 4. Local density of states for the valence band of the 14-layer Si(111)Cl film for the Cl overlayer (a); for the Cl plus the first (adjacent) Si layer (b); and for the sum of the Cl, the first Si, and the second Si layer (c). The zero energy corresponds to the vacuum level.

B. Lower conduction band

Before extending our LDS calculation to the conduction band, it is advisable to ascertain how well one can describe the conduction states by means of the 13-function basis set. To this end we have calculated the conduction-band DOS for the bulk Si crystal using the 13-function set as well as an extended set consisting of the 13 functions plus four s-type and four p-type single Gaussians of expo-

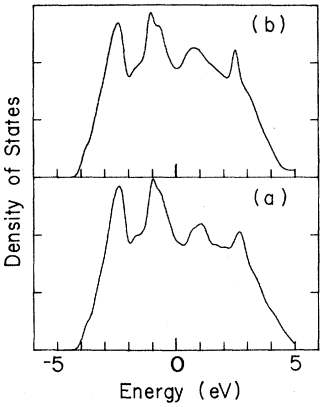

FIG. 5. Conduction-band density of states of the bulk Si crystal calculated by using the 13-function basis set (a) and by using the extended basis (b). The zero energy corresponds to the vacuum level.

nents 0.257 644, 0.503 922, 1.452 21, and 3.937 14. The results are presented in Fig. 5. Up to the vacuum level ($E=0$) the DOS obtained from the 13-function set agree well with that from the extended basis. Thus one can be quite confident about using the 13-function set to study the part of the conduction band below the vacuum level (referred to as the lower conduction band) for the chemisorbed surface. The LDS calculated for the Cl layer, for the Cl layer plus the next Si layer, and for the Cl layer plus the next two Si layers are shown in Fig. 6. The peak at −3.4 eV may be associated with adsorption, whereas the two peaks at −2.3 and −1.0 eV are essentially due to bulk states because they are absent in the Cl-layer LDS and because they appear at the same energies in the DOS of the bulk crystal (Fig. 5). It is stated in Ref. 21 that a Cl-induced transition (electron-energy-loss data) observed for Si(111) 7 × 7 has the final state 2.3 eV above the top of the valence band. This is equivalent to 3.2 eV below the vacuum level if we use the experimental value of 5.5 eV for the energy difference between the vacuum level and the top of the valence band. We see that this state at −3.2 eV is close to our calculated peak at −3.4 eV.

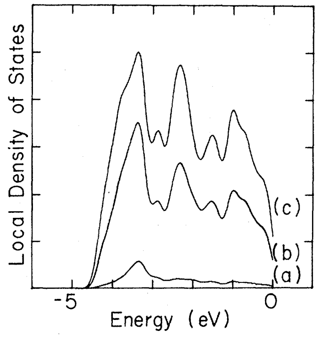

FIG. 6. Local density of states for the lower conduction band of the 14-layer Si(111)Cl film for the Cl overlayer (a); for the Cl plus the first (adjacent) Si layer (b); and for the sum of the Cl, the first Si, and the second Si layer (c). The zero energy corresponds to the vacuum level.

The −3.4-eV peak consists of energy levels from a group of $\vec{k}_{\parallel}$ points including $\overline{\Gamma}$. In the $\overline{\Gamma}$ wave function, the 3*s* and 3*pz* orbitals on the Cl atom have their relative phase so as to be pointing inward whereas the hybridized 3*s*-3*pz* orbitals on the adjacent Si atoms point toward the Cl layer. The Cl and the neighboring Si are antibonding with a larger amplitude on Si. The population-analysis calculation shows that the fractional charge allocated to the Cl layer is considerably smaller than those to the next few layers of Si. Outside the $\overline{\Gamma}$ point, some *px*, *py* admixture sets in, but the individual atomic constituents by and large remain primarily *s*-*pz*-like with strong cancellation between the Cl and adjacent Si atoms. Although the Cl valence orbitals include both 3*s*, 3*p* and the *s*′, *p*′ supplement, the *s*′, *p*′ components in the wave functions are small compared to 3*s*, 3*p*. Hence we can roughly characterize the −3.5-eV peak as a σ-type antibonding state between Cl and Si.

C. Estimation of LDS for the upper conduction band

Rowe *et al.* have observed some peaks in their photoemission spectra corresponding to states above the vacuum levels.[21] This makes the study of the upper conduction band (the part above the vacuum level) especially interesting. However, one cannot expect to obtain very accurate results for these high conduction states using the 13-function basis set. One can, of course, supplement it by single Gaussians, including those on floating sites outside the film. While this procedure has been fruitful for bulk crystals, application to the thin-film problem would make the size of the secular equation too large to handle with our local computing facility. Nevertheless, we notice that in the case of the bulk crystal the 13-function set gives an upper-conduction-band DOS which still shows good resemblance to the one deduced from the extended basis set. For this reason we endeavor to carry the 13-function calculation even above the vacuum level. It must be emphasized that the LDS curves for the upper conduction band of the chemisorbed film, which is shown in Fig. 7, should be regarded only as a theoretical estimate for qualitative purposes. In spite of this reservation, the LDS curves do reveal some interesting features. The two peaks at 3.7 and 4.7 eV are clearly Cl related as they undergo little change

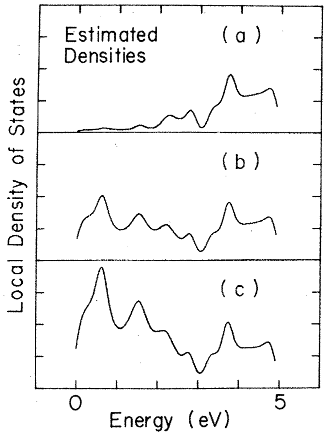

FIG. 7. Estimated local density of states for the upper conduction band of the 14-layer Si(111)Cl film for the Cl overlayer (a); for the Cl plus the first (adjacent) Si layer (b); and for the sum of the Cl, the first Si, and the second Si layer (c). The zero energy corresponds to the vacuum level.

from Fig. 7(a) to Fig. 7(c). They are very close to the experimental data labeled as β and γ which, referred to the vacuum level, have energies 3.4 and 4.8 eV, respectively. The nearly exact agreement, of course, is fortuitous; nevertheless, the overall correspondence between the LDS and the observed peaks is interesting. The LDS for the adsorbate layer alone [(Fig. 7(a)] exhibits a structure at 2.2–2.9 eV, but it disappears as the contribution from the adjacent substrate layers are added. Instead a broad structure at 0.5–1.7 eV evolved; it is reminiscent of the one at the same energy range for the bulk Si crystal as shown in Fig. 5. Hence this is largely a bulk-state effect. The α peak observed by Rowe *et al.*[21] is at 1.0 eV above the vacuum level but is not quite as broad.

We have also analyzed the nature of the states in the 3.7- and 4.7-eV peaks. None of them belong to $\bar{\Gamma}$, yet for most states the Cl components have more s, pz than px, py constituents. Furthermore they are antibonding states between Cl and Si. These states distribute over a wide region which covers the 3.7–4.7-eV double peak. In some ways they are similar to the states near the –3.5-eV peak described in Sec. V B. However, the 3.7–4.7-eV states have much higher localization at the Cl atoms than do the –3.5 eV-states. Furthermore, the Cl orbitals in the 3.7–4.7-eV wave functions contain more s', p' than $3s, 3p$ components, in contrast to the –3.5-eV states which are predominantly $3s$-$3p$ type. Thus we regard the 3.7–4.7-eV states as a set of higher σ-type antibonding states. It is almost tempting to introduce the name $4s$-$4p$-σ antibonding states, but the atomic $4s, 4p$ states of Cl are so much distorted in the solid that they do not offer a realistic description. We may add that the Si orbitals, unlike the Cl ones, are still mainly $3s, 3p$ with only modest s', p' admixture. One can understand this because the totality of all the Si $3s, 3p$ states span enough conduction states so that some of them can interact with the Cl "$4s$-$4p$" states, whereas the s', p' orbitals are absolutely needed to form the "$n=4$" Cl orbitals. This explanation also suggests that the 13-function set may be too limited to accurately reproduce the "$n=4$" states. When more basis functions are added to strengthen the variational freedom, the energies of some of the higher σ antibonding states may decrease appreciably. Hence, high accuracy cannot be claimed for the 3.7–4.7 eV region; in fact the shape of the double peak may change substantially (or may even merge) as the calculation is refined.

VI. DISCUSSION

We have presented here a self-consistent LCAO calculation of the electronic structure of the Si(111)Cl surface. The general method is essentially an extension of the one developed for bulk crystals. The basis set includes the minimal $1s, \ldots, 3p$ orbitals plus an extra s-type and an extra p-type function, so that it has sufficient variational freedom to accurately reproduce the occupied states as well as the lower conduction-band states. The resulting LDS for these two kinds of states are in good agreement with experiment. Our calculation also gives the energies of the higher conduction states, but they are of lower accuracy. Because of the possibility of experimentally probing the conduction states above the vacuum level, it would be desirable to perfect the LCAO scheme for those high states. This can be done by supplementing the basis sets with several sets of single Gaussians, since in the case of bulk crystals accurate energies for the highly excited states have been obtained by the single-Gaussian technique.[33] For a 14-layer thin film, each single Gaussian (including s and p type) gives rise to 56 basis functions. This puts a serious limit on the number of single Gaussians that can be accommodated. However, by orthogonalizing the $3s, 3p, s'$, p', and single-Gaussian Bloch sums to all the $1s$, $2s$, and $2p$ core Bloch sums, the latter can be deleted from the basis set. Using the orthogonalization technique, it should be possible to handle a basis set containing $3s, 3p, s', p'$, plus three or four different single Gaussians (s and p type) with a computer of very large core memory. Alternatively the basis functions may be distributed differently among different layers. For instance, one may allocate more variational freedom to the outer layers than to the interior layers or even introduce floating sites outside the film.

The selection of the exchange parameter α deserves some comments. Let us first review some SCF electronic calculations for bulk crystals and atoms in this regard. In a series of OPW studies for Si and III–V compounds,[38,43] band gaps derived from $\alpha = 1$ are found to be in good agreement with experiments whereas $\alpha = \frac{2}{3}$ gives too small gaps. (It is interesting to note[38,43] that if one adopts the OAP approximation instead of going to self-consistency, then $\alpha = \frac{2}{3}$ gives better results than $\alpha = 1$.) Energies were expressed relative to the top of the valence band (rather than to the vacuum level) in those works. On the other hand, $\alpha = \frac{2}{3}$ has been used successfully for alkali metals,[3] aluminum,[8] and transition elements.[4,6] A slightly lower value ($\alpha = 0.64$) was selected for iron.[5] For free atoms the combination of α in the range of 0.69 to 0.77 (depending on Z) with the Slater method of transition states works well for excitation and ionization energies.[44] In case the transition-state technique is not used, $\alpha = 1$ is preferable.

If we are mainly interested in the structure of the valence and conduction bands, $\alpha = 1$ would be the right choice. Indeed our calculated band gap for bulk Si with $\alpha = 1$ (1.43 eV using the 13-function set and 1.37 eV using an extended set), though slightly higher than the experimental value, is quite satisfactory. However, $\alpha = 1$ places the valence band of the bulk crystal 1 eV too low relative to the vacuum level (Sec. II). For bulk-crystal studies energy-level differences rather than absolute energies are of major concern, but the vacuum level plays a much more important role in surface problems. Since the valence-band edges are only slightly distorted in going from the bulk crystal to the surface case, the 1-eV discrepancy for $\alpha = 1$ would appear also in Si(111)Cl. This not only suppresses the valence band but also may alter the interaction between the surface and bulk states. Consequently we select $\alpha = 0.9$ for Si. As to Cl we use atomic calculations as a guide. Since our calculation for Si(111)Cl is not of the transition-state type, $\alpha = 1$ is used for Cl in this paper. As a test we have repeated the thin-film calculation keeping $\alpha = 0.9$ for Si but changing α to 0.95 for Cl. The surfacelike eigenvalues derived from the initial crystal potential (Sec. III B) differ substantially from the corresponding ones with $\alpha(\mathrm{Cl}) = 1.0$, but as self-consistency is reached, the two sets of energy spectra become more alike. The two Cl-related peaks in the valence-band LDS, for example, are at 10.9 and 13.2 eV for $\alpha(\mathrm{Cl}) = 0.95$. Thus our approach is to choose the exchange parameter for the substrate by the criterion of the vacuum level and use free-atom calculations as a guide for selecting α for the adsorbate. The calculated energies of the substrate-adsorbate system do not appear to depend very sensitively on the α value of the adsorbate.

It is not necessary to confine oneself to the $X\alpha$ version of the statistical exchange approximation. For example, the Wigner interpolation form is used by Appelbaum and Hamann.[20,27] In a recent paper on the energy bands of ferromagnetic nickel (bulk), Wang and Callaway explicitly introduced some correlation effects by using the exchange-correlation potential of von Barth and Hedin in place of the Kohn-Sham-Gaspar exchange approximation.[4] Undoubtedly the optimal value of α as gauged by the vacuum level would vary depending on the particular form of the exchange or exchange-correlation potential adopted. It would be very desirable to study how these various approximations affect the vacuum-level energies of the bulk crystal and the free-atom energies so as to arrive at a more unified version of the exchange-exchange-correlation potential.

ACKNOWLEDGMENTS

The authors wish to thank Dr. J. E. Rowe for calling their attention to the Si(111)Cl system when they were at the initial stage of extending the LCAO scheme to study surface adsorption and for keeping them informed of his experimental results prior to publication. They were also benefited by helpful discussions with Professor M. B. Webb. Special appreciation must be extended to Dr. W. P. Menzel for providing the computer program for multicenter integration involving Eq. (6), which is most essential for this work, and to Professor E. E. Lafon for the use of some of his programs for bulk-crystal calculations. This work was supported in part by the NSF. Preliminary accounts of this work have been given in Ref. 45.

---

[1] E. E. Lafon and C. C. Lin, Phys. Rev. 152, 579 (1966).

[2] R. C. Chaney, T. K. Tung, C. C. Lin, and E. E. Lafon, J. Chem. Phys. 52, 361 (1970).

[3] W. Y. Ching and J. Callaway, Phys. Rev. Lett. 30, 441 (1973); Phys. Rev. B 11, 1324 (1975); 9, 5115 (1974).

[4] C. S. Wang and J. Callaway, Phys. Rev. B 15, 298 (1977); 9, 4897 (1974).

[5] R. A. Tawil and J. Callaway, Phys. Rev. B 7, 4242 (1973).

[6] J. Rath and J. Callaway, Phys. Rev. B 8, 5398 (1974).

[7] R. C. Chaney, C. C. Lin, and E. E. Lafon, Phys. Rev. B 3, 459 (1971).

[8] S. P. Singhal and J. Callaway, Phys. Rev. B 16, 1744 (1977).

[9] U. Seth and R. Chaney, Phys. Rev. B 12, 5923 (1975).

[10] R. C. Chaney, E. E. Lafon, and C. C. Lin, Phys. Rev. B 4, 2734 (1971).

[11] J. E. Falk and R. J. Fleming, J. Phys. C 6, 2954 (1973).

[12] R. C. Chaney and C. C. Lin, Phys. Rev. B 13, 843 (1976).

[13] R. C. Chaney, Phys. Rev. B 14, 4578 (1976).

[14] W. Y. Ching, C. C. Lin, D. L. Huber, Phys. Rev. B 14, 620 (1976).

[15] W. Y. Ching, C. C. Lin, and L. Guttman, Phys. Rev. B 16, 5488 (1977).

[16] I. Shavitt, in *Methods of Computational Physics*, edited by B. Alder, S. Fernbach, and M. Rotenberg (Academic, New York, 1963), Vol. 2, p. 1.

[17] W. Y. Ching and C. C. Lin, Phys. Rev. B 12, 5536 (1975).

[18] J. Callaway and J. L. Fry, in *Computational Methods in Band Theory*, edited by P. M. Marcus, J. F. Janak, and A. R. Williams (Plenum, New York, 1971), p. 512.

[19] M. Singh, C. S. Wang, and J. Callaway, Phys. Rev. B 11, 287 (1975).

[20] J. A. Appelbaum and D. R. Hamann, Rev. Mod. Phys. 48, 479 (1976).

[21] J. E. Rowe, G. Margaritondo, and S. B. Christman, Phys. Rev. B 16, 1581 (1977).

[22] M. Schluter, J. E. Rowe, G. Margaritondo, T. M. Ho, and M. L. Cohen, Phys. Rev. Lett. 37, 1632 (1976).

[23] J. A. Appelbaum and D. R. Hamann, Phys. Rev. B 6, 2166 (1972); Phys. Rev. Lett. 31, 106 (1973); 32, 225 (1974).

[24] G. P. Alldredge and L. Kleinman, Phys. Rev. Lett. 28, 1264 (1972); Phys. Rev. B 10, 559 (1974); Phys. Lett. A 48, 337 (1974).

[25] J. G. Gay, J. R. Smith, and F. J. Arlinghaus, Phys. Rev. Lett. 38, 561 (1977).

[26] S. Ciraci and I. P. Batra, Phys. Rev. B 15, 3254 (1977).

[27] J. A. Appelbaum and D. R. Hamann, Phys. Rev. Lett. 34, 806 (1975).

[28] R. V. Kasowski, Phys. Rev. Lett. 33, 1174 (1974); 37, 219 (1976).

[29] K. Hirabayashi, J. Phys. Soc. Jpn. 27, 1475 (1969).

[30] K. C. Pandey and J. C. Phillips, Phys. Rev. Lett. 32, 1433 (1974); Solid State Commun. 14, 439 (1974).

[31] K. C. Pandey, Phys. Rev. B 14, 1557 (1976).

[32] K. C. Pandey, T. Sakurai, and H. D. Hagstrum, Phys. Rev. B 16, 3648 (1977).

[33] J. E. Simmons, C. C. Lin, D. F. Fouquet, E. E. Lafon, and R. C. Chaney, J. Phys. C 8, 1549 (1975).

[34] E. Clementi and D. R. Davis, J. Comp. Phys. 1, 223 (1966).

[35] These Gaussian exponents were taken from the atomic SCF calculation by A. Veillard, Theor. Chim. Acta (Berlin) 12, 405 (1968).

[36] F. G. Allen and G. W. Gobeli, Phys. Rev. 127, 150 (1962).

[37] G. G. Macfarlane, T. P. McLean, J. E. Quarrington, and V. Roberts, Phys. Rev. 111, 1245 (1958).

[38] D. J. Stukel and R. N. Euwema, Phys. Rev. B 1, 1635 (1970).

[39] B. Bak, J. Bruhn, and J. Rastrup-Andersen, J. Chem. Phys. 21, 753L (1953); R. C. Mockler, J. H. Bailey, and W. Gordy, J. Chem. Phys. 21, 1710 (1953); Y. Morino and E. Hirota, J. Chem. Phys. 28, 185 (1958).

[40] In Eq. (17) the z axis is normal to the surface. Referred to the cubic axes, the four angular factors in Eq. (17) are $x+y+z$, $xy+xz+yz$, xyz, and $x^3+y^3+z^3-(\frac{3}{5})(x+y+z)r^2$.

[41] See, for example, J. C. Slater and K. H. Johnson, Phys. Rev. B 5, 844 (1972); J. W. D. Connolly, J. Chem. Phys. 58, 4265 (1973); J. G. Norman, J. Chem. Phys. 61, 4630 (1974).

[42] R. S. Mulliken, J. Chem. Phys. 23, 1833, 1841 (1955); 36, 3428 (1962).

[43] See D. J. Stukel and R. N. Euwema, Phys. Rev. 188, 1193 (1969); T. C. Collins, D. J. Stukel, and R. N. Euwema, Phys. Rev. B 1, 724 (1970).

[44] J. C. Slater, *Quantum Theory of Molecules and Solids* (McGraw-Hill, New York, 1974), Vol. 4.

[45] K. Mednick and C. C. Lin, Bull. Am. Phys. Soc. 21, 305, 937 (1976).